DOI: https://doi.org/10.61762/pjstvol7iss2art002

PLATFORM - A Journal of Science & Technology

Received: 29 November 2024, Revised: 15 December 2024, Accepted: 27 December 2024, Published: 31 December 2024, Publisher: UTP Press, Creative Commons: CC BY 4.0

CATALYTIC CO-GASIFICATION OF SUGARCANE BAGASSE AND OIL PALM FROND FOR H_2-RICH SYNGAS PRODUCTION

Ezza Faiharah*, Noorfidza Yub Harun[1]

[1]Department of Chemical Engineering, Universiti Teknologi PETRONAS, Malaysia

*Email: ezzafaiharah17@gmail.com

ABSTRACT

Syngas, primarily consisting of hydrogen and carbon monoxide, offer a cleaner substitute for fossil fuels and can be produced through co-gasification of biomass waste. This study investigates sugarcane bagasse (SB) co-gasification and oil palm frond (OPF). The objective was to investigate the influence of parameters (temperature, biomass ratio and catalyst) and optimise process parameters for enhanced syngas production. The feedstock sample was placed in a fixed bed horizontal tube furnace reactor, and the gaseous product was sent to GC-NGA for analysis. Thirty-four experiments, indicated from RSM software, were conducted and syngas composition, considering factors such as temperature (700°C to 900°C), biomass ratio (20SB:80OPF, 50SB:50OPF, and 80SB:20OPF), and catalyst loading (0wt%, 15wt%, and 30wt%). ANOVA analysis showed P-value and F-values of limestone and dolomite response on H_2 and syngas were obtained in the range $P < 0.0001$ and 50.99-112.55, respectively, indicating the model was significant. The model-predicted data proved to approach the actual data with high accuracy as all R^2 values were in the range of 0.98-0.99, which was closer to one. The results showed the strong influence of the process temperature on H_2 and Syngas yield, followed by the catalyst loading and biomass ratio. The highest H_2 yield of 25 vol% and syngas of 49 vol% were produced during catalytic co-gasification of the 20SB:80OPF ratio with limestone, followed by dolomite (24 vol% and 41 vol%, respectively) at 900°C. In conclusion, the study revealed that both catalysts enhance the production of H_2-rich syngas, with limestone proving to be the superior catalyst.

Keywords: *Biomass waste, co-gasification, response surface methodology, syngas*

INTRODUCTION

Background

In the current trend of industrial development, the primary goal is no longer solely focused on achieving economic gains. The urgent global issues surrounding carbon dioxide levels in the atmosphere, climate change, and recycling waste have become significant motivators for seeking commodities derived from alternative non-fossil sources. In United Nations Conference 2015, The Sustainable Development Goals (SDG) were declared as a key pillar of 2030 sustainable development. Syngas, mainly composed of H_2 and CO, can be used as a cleaner alternative to fossil fuels in various applications, providing a route to diminish greenhouse gas emissions and alleviate the effects of climate change. Syngas serves in the creation of chemicals like methanol and ammonia and also holds potential for transformation into synthetic hydrocarbons via variation synthesis, which can subsequently undergo refinement into liquid fuels like diesel and jet fuel [1]. Syngas-based fuels such as synthetic diesel or synthetic natural gas (SNG) can be used as alternatives to conventional fossil fuels in transportation [2]. Hydrogen is a versatile energy carrier that can be used in fuel cells for zero-emission transportation or stationary power generation. Syngas can be blended with biogas derived from organic waste or biomass to produce a cleaner-burning fuel with higher energy content.

Co-gasification is a process that involves converting multiple feedstocks, such as coal, biomass, or waste materials, into syngas. This process offers advantages

over standalone gasification of individual feedstocks as it allows for more efficient utilisation of resources because different feedstocks can complement weaknesses and enhance overall gasification performance. Blending biomass with coal, plastic, or sewage sludge for co-gasification addresses the challenges encountered when gasifying single feedstocks [3]. Co-gasification can also lead to environmental benefits by reducing greenhouse gas emissions and mitigating the environmental impacts associated with waste disposal. Process waste consists of residues generated during crop processing, which can be repurposed into valuable resources such as husks, seeds, roots, pulps, straw, stubble, bagasse, and molasses [4]. Utilisation of biomass from industry and agriculture has emerged as the next innovation in power generation because the reliance on non-renewable fossil fuels decreased [5]. Over 160 million tonnes of biomass are produced in Malaysia annually, acting as a potential source of bioenergy and a sustainable solution to fulfill the country's energy requirements [6]. Over the past decade, Malaysia has consistently held the top spot as the global manufacturer and supplier of palm oil. The tropical climate of Malaysia facilitates the production, expansion, and advancement of oil palm cultivation in the country [7].

Natural catalysts are renewable, biodegradable, and often exhibit high specificity, longevity and efficiency, which can result in lower overall process costs. The study by Bo et al. [8] investigated the activity of natural catalyst (dolomite, limestone, and NiO/dolomite) in the context of hydrogen generation through biomass gasification and discovered that the optimal hydrogen yield reached 510 ml/g. In gasification processes, natural catalysts can help to enhance the water-gas shift reaction kinetics, shows high hydrogen yields as result [9]. Natural catalysts can accommodate a wide range of feedstocks, including biomass, organic wastes, and agricultural residues. This versatility allows for flexibility in feedstock selection, enabling the utilisation of diverse and sustainable raw materials for hydrogen production. Catalyst is employed to expedite the reaction rate and enhance the production of H_2 yield. Alkali metals, dolomites, and nickel (Ni) are the common catalysts utilised in biomass steam gasification [10]. The mineral dolomite is found in the form of $CaMg(CO_3)_2$ while limestone has the same general formula as dolomite, which is $CaCO_3$. Dolomite and limestone catalysts are widely available and inexpensive compared to metallic and Ni-based catalysts [11].

Oil palm fronds (OPF) are typically left on the ground between palm trees in substantial quantities for natural decomposition, serving purposes such as soil conservation, erosion control, and nutrient recycling [12]. With a low sulphur content (11%), OPF emissions have a reduced environmental impact, as sulphur have the potential to react with water, oxygen, and oxidants to form acidic compounds [12]. According to Venkatesh et al. [13], in the study of gasification of coconut shells and sugarcane bagasse, coconut shells give a low gas production rate (1.4724 m^3/hr) and low gasification efficiency (46.96%), while sugarcane bagasse material gives high gas production rate (1.5535 m^3/hr) and high gasification efficiency (52.86%). Hence, the co-gasification of oil palm frond and sugarcane bagasse is expected to have high syngas yields while also presenting environmentally favourable characteristics. Dolomite and limestone can enhance the reactivity of the gasification process by providing catalytic sites for the reactions involved, such as the reforming of hydrocarbons [14]. Besides, these natural catalysts also act as heat sinks, helping to smooth the temperature fluctuations within the gasification reactor. This increases the efficiency of the product yield while reducing the risk of thermal stress on the reactor performance [15].

In the present study, the co-gasification of biomass waste, specifically oil palm fronds and sugarcane bagasse, was conducted in a fixed-bed horizontal tube furnace reactor. The effects of varying blending ratios, temperature, and catalysts on the quality of syngas were examined, and the optimisation of process parameters was carried out to achieve hydrogen-rich syngas production.

Gasification of Biomass

Gasification is a thermochemical process that converts solid biomass into combustible gaseous fuel known as "Synthesis gas," or Syngas, with a limit or sub-stoichiometric air supply [16]. This process is used to extract energy from biomass, such as municipal solid waste, tyres, biomass waste, and coal [17]. The gasification process includes four zones: the drying zone, the pyrolysis zone, the combustion zone, and the reduction zone.

Drying Zone

The drying process was critical for removing surface water through filtration, evaporation, or a combination of both methods. The moisture content began to evaporate as the drying module's temperature rose from the starting point (To = 298 K) to 368 K. The amount of moisture present in biomass typically ranges from 5% to 35%, depending on its type, and at a temperature of about 100°C, it transformed into steam [18]. The majority of gasification processes utilize feedstock containing moisture levels ranging from 10 to 20% to generate fuel gas with elevated heating value [19].

Pyrolysis Zone

Pyrolysis involves heating feedstock to a specified maximum temperature and maintaining it for a duration without introducing oxygen. Pyrolysis is an endothermic process that requires heat to initiate the chemical reaction yielding syngas [20]. This process yields solid charcoal, liquid tar, and gas, with the proportions of these products determined by the characteristics of the biomass feedstock utilised [18]. The process of pyrolysis, which converts hydrocarbons into tar, occur at temperatures ranging from 125°C to 500°C for biomass feedstock.

Combustion Zone

Combustion is an endothermic process facilitated by the presence of oxygen as a supporting agent, resulting primarily in the production of heat and CO_2 as combustion products [20]. The combustion process is essential for minimising the number of tars generated during combustion. Heterogeneous interactions between solid carbonised fuel and atmospheric oxygen occur in this zone, producingarbon dioxide and a significant quantity of heat [18]. Moreover, hydrogen and oxygen combine to form water vapour.

Reduction Zone

The reduction zone is the main gasification reaction, where the thermochemical breakdown of the lignocellulosic component results in the formation of char and volatiles. Within the reduction zone, the sensible heat of gases and charcoal is converted into the chemical energy of the producer gas produced when high-temperature chemical reactions occur. The endothermic reaction process generates combustible products such as, CO, H_2, and CH_4[20].

METHODOLOGY

Material Preparations and Characterisation

Sugarcane bagasse (SB) and oil palm fronds (OPF) were used as feedstock in this study. The SB was collected from sugarcane juice stalls and OPF from palm oil plantation FELCRA Nasaruddin Sdn Bhd Bota, Perak. The feedstock was divided into two parts. Firstly, the feedstock was prepared for characterisation and for catalytic co-gasification experiments. SB and OPF were chopped into 1-2-inch sizes, as shown in Figure 1. After that, the feedstocks were dried in an oven at a temperature of 100-105°C for 24 hours to remove the inherent moisture content. The biomass was grinded and sieved to 1-2 mm for ultimate analysis and calorific value determination [3]. Ultimate analysis of biomass was performed using the CHNS analyser, and the calorific value was determined using bomb calorimeter. Table 1 shows the SB and OPF mechanically mixed into different biomass blending ratios, which were SB20:OPF80, SB50:OPF50 and SB80:OPF20.

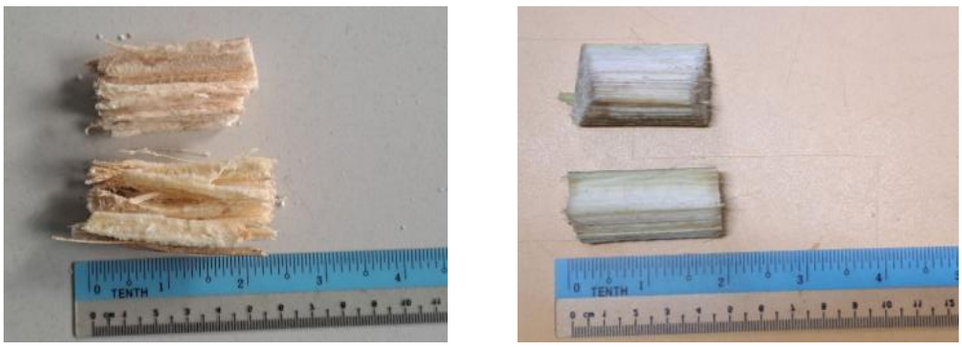

Figure 1 Small pieces of SB and OPF

Natural mineral catalysts used in this study were dolomite and limestone, as shown in Figure 2. The natural catalyst were calcined at 900°C for 4 hours [3]. The catalyst loading varied, with composition of 0 wt%, 15 wt% and 30 wt%. The catalysts were characterised using Brunner-Emmet-Teller (BET) surface area, pore size, and pore volume. X-ray Fluorescence (XRF) was used to identify the chemical composition of catalysts, as shown in Table 2.

Figure 2 Natural catalyst (dolomite & limestone)

Table 1 Ultimate analysis and calorific value for each sample

Sample	Ultimate analysis				HHV (MJ/kg)
	C [%]	H [%]	N [%]	S [%]	
SB	43.86	5.698	8.94	0.117	17.33
OPF	41.82	6.235	10.11	0.109	15.92
20SB 80OPF	41.03	6.199	11.84	0.094	16.01
50SB 50OPF	44.15	6.352	11.92	0.076	16.44
80SB 20OOF	42.43	6.384	15.74	0.044	16.78

Table 2 Compound composition of feedstock and catalyst using XRF (wt%)

Compound	20SB:80OPF	50SB:50OPF	80SB:20OPF	Dolomite	Limestone
K_2O	53.22	43.2	37.6	-	0.111
CaO	18.3	23.8	26.4	61.6	92.2
SiO_2	5.22	8.79	9.59	0.16	1.34
SO_3	2.46	5.94	7.59	0.062	0.0775
P_2O_5	2.07	3.36	4.3	-	0.062
Fe_2O_3	1.07	1.99	2.17	0.114	0.32
Al_2O_3	-	-	0.37	0.12	0.822
MnO	0.29	-	-	0.01	0.02
ZnO	0.099	0.23	0.25	-	0.008
NiO	-	0.185	-	-	-
CuO	-	0.28	0.38	-	-
MgO	1.1	1.9	2.2	37.86	4.99
Cl	15.9	10.3	9.15	0.0346	-
Br	0.11	-	-	-	-
MoO_3	0.1	-	-	-	0.006
Rb_2O	0.011	-	-	-	-
NiO	-	0.19	-	-	-
SrO	-	-	-	0.0132	0.032
ZrO_2	-	-	-	0.001	0
TiO_2	-	-	-	-	0.058

Table 3 Optimisation for catalytic co-gasification of SB and OPF

Parameters	Goal	Lower limit	Upper limit
Temperature (°C)	In range	700	900
Biomass ratio (wt.%)	In range	20:80	80:20
Catalyst loading (wt.%)	In range	0	30
Hydrogen production (vol.%)	Max	-	-
Syngas production (vol%)	Max	-	-

Experimental Design – Response Methodology Surface

Response Surface Methodology (RSM), in conjunction with the standard Box-Behnken Design (BBD) technique, was utilised to design a series of experiments for catalytic co-gasification, and this technique was crucial for analysing the effective variables to optimise their response to desired outputs. By employing statistical analysis, this tool investigated the interaction and effect of factors on the desired outcome [21]. RSM created a surface that relates input and output variables, allowing for the investigation of interactions among variables [3]. Three input variables— operating temperature of co-gasification (A), catalyst loading (B), and blending ratio (C)— were identified at three different levels using BBD. The upper and lower boundaries of these input variables were determined based on preliminary results and experimental setup limitations in Table 3. Temperature, catalyst loading, and blending ratio ranges were set to 700-900°C, 0-30 wt%, and 20-80 wt%, respectively. For each run of the experiment, the weight of feedstock used was 1 g.

Experimental Procedure

The experiment was executed in a fixed bed horizontal tube furnace reactor, as shown in Figure 3. According to Abioye et al. [21], the reactor operates in four sequential steps: (i) The reactor was filled with 1g of 20SB:80OPF in a ceramic boat, and the ceramic tube was sealed. (ii) N_2 was purged into the reactor with a 10 mL/min flow rate for 10 minutes to eliminate any trapped gas molecules. (iii) The heating element was used to achieve the desired temperatures for the experiment. (iv) Once the desired temperature is achieved, the reaction stabilises for the specified holding duration before completion. The reaction was held steady for 10 minutes once the desired furnace temperature reached. The gaseous products from the co-gasification process exited the reactor and flowed through a gas cooling system consisting of a coiled stainless-steel tube submerged in an ice bath. Subsequently, the cooled gas was gathered at a sampling location for analysis using Gas Chromatography Natural Gas Analyzer (GC-NGA). The analysis with GC-NGA was repeated three times, and the average value was taken to ensure the accuracy of the result. After the reactor cooled down, the air flow was disconnected, and the equipment was switched off.

Brunauer-Emmett-Teller (BET) Analysis

The isotherm plot represented the adsorption behaviour of limestone and dolomite as a function of

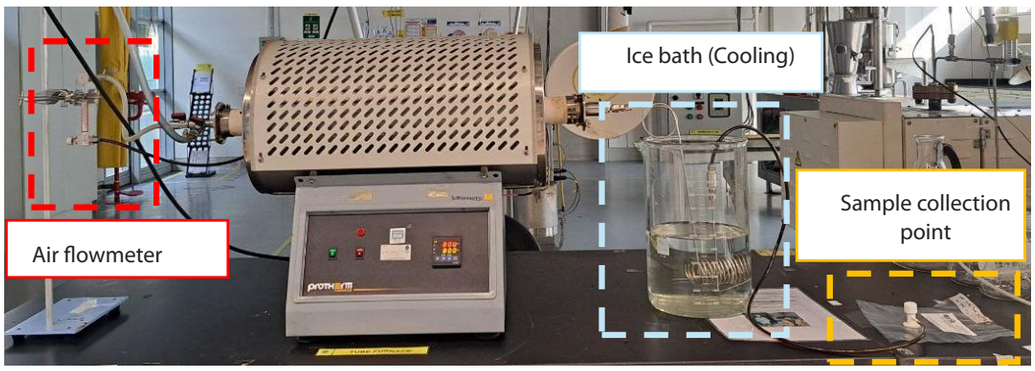

Figure 3 Experimental setup

relative pressure (P/Po) shown in Figure 4. The x-axis represents the relative pressure (P/Po), while the y-axis represents the quantity adsorbed, measured at standard temperature and pressure (cm^3/g STP) per gram of adsorbent. Both limestone and dolomite exhibit an increase in the quantity adsorbed as the relative pressure increases. Dolomite shows a higher quantity of adsorbed compared to limestone across all relative pressures. At low relative pressures (P/Po < 0.2), both materials show a relatively small amount of gas adsorption, and it can be observed that dolomite starts adsorbing gas slightly more than limestone in this region. At high-pressure region (P/Po > 0.7), dolomite continues to adsorb more gas than limestone, and the difference becomes more pronounced at higher pressures.

The higher adsorption capacity of dolomite compared to limestone indicates that dolomite has a higher surface area or more active sites available for gas adsorption, as shown in Figure 5. This makes dolomite a more effective adsorbent under the given conditions than limestone. Dolomite has a steeper slope and a lower intercept compared to limestone, which typically indicates that dolomite has a higher specific surface area compared to limestone, as the specific surface area is inversely proportional to the y-intercept and directly proportional to the slope of the line in the BET plot. However, a higher surface area does not necessarily mean a better catalyst for hydrogen production in gasification, as the catalytic activity is also influenced by the chemical composition and the specific active sites available on the material [22]. K_2O, CaO, SiO_2, Fe_2O_3, and MgO, which are characterised as metallic oxides,

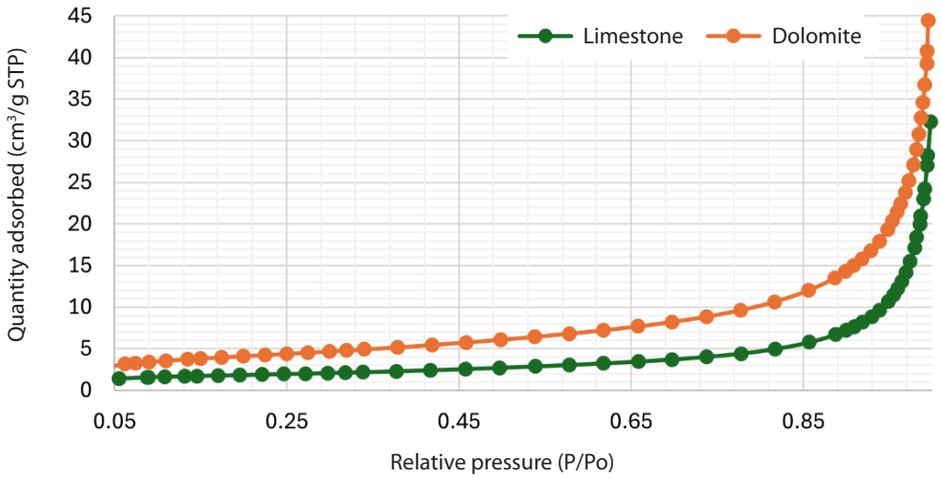

Figure 4 Isotherm linear plot of calcined limestone and dolomite

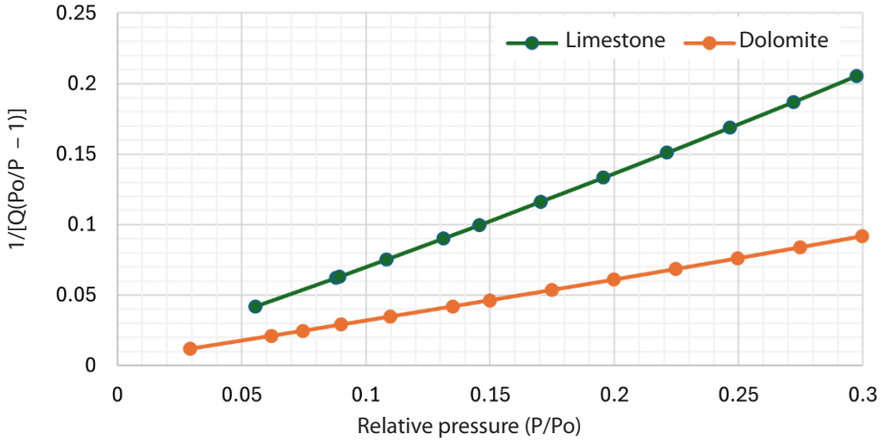

Figure 5 BET surface area plot of calcined limestone and dolomite

were present in all three feedstocks. The compound that presents in highest percentage for each ratio is K_2O and 20SB:80OPF has the highest percentage of 53.2%. Dolomite and limestone both contain CaO as the most compound, 61.6% and 92.2% respectively. A mixture of biomass and CaO-based sorbent will enhance hydrogen production yield [23].

RESULTS AND DISCUSSION

ANOVA Analysis and Equation of Regression

RSM and BBD were used to develop the statistical relationship between the actual values of variables and the experimental response of H_2 and Syngas. Table 4 shows the experimental results based on the model generated by RSM. The significance of the model and its terms was determined by a higher F-value and a lower probability value. A P-value of less than 0.05 (indicating a 95% confidence level) shows that the model terms are significant and closely match the actual experimental results. The regression analysis assisted in finding the best-fit quadratic model for the experimental results, as shown in Table 5. The correlation equation shows the relationship between the process variables and their mutual interaction effect on the responses.

ANOVA analysis was performed to determine the significance of the model and variables for H_2 and syngas, as shown in Table 6. P-value and F-values of limestone and dolomite response on H_2 and syngas were obtained in the $P < 0.0001$ and 50.99-112.55 range, respectively. A lower P-values, that less than 0.0500 and higher F-values indicates the model was significant. The model predicted data proved to approach the actual

Table 4 Experimental design results

Run	A: Temperature (°C)	B: Biomass Ratio (SB:OPF)	C: Catalyst (wt.%)	Std. Run	Limestone		Dolomite	
					H_2 (Vol.%)	Syngas (Vol.%)	H_2 (Vol.%)	Syngas (Vol.%)
1	800	80;20	30	12	14	27	18	30
2	700	50;50	0	5	2	10	2	10
3	800	50;50	15	15	16	27	18	90
4	800	20;80	0	9	12	24	12	24
5	900	50;50	0	6	22	37	22	37
6	700	20;80	15	1	9	18	7	15
7	900	20;80	15	2	25	49	22	44
8	700	80;20	15	3	8	17	4	14
9	900	80;20	15	4	24	43	24	41
10	800	20;80	30	11	17	31	14	24
11	800	50;50	15	16	17	30	18	28
12	800	50;50	15	13	17	27	19	31
13	800	50;50	15	17	17	31	20	31
14	800	80;20	0	10	14	24	14	24
15	700	50;50	30	7	11	19	7	14
16	900	50;50	30	8	23	46	22	39
17	800	50;50	15	14	17	30	18	28

Table 5 The mathematical relationship with process variables based on ANOVA for H_2 and syngas

Catalysts	Correlation equation in terms of coded factors
Limestone	$H_2 = 16.80 + 8.00\ A - 0.3750\ B + 1.88\ C + 0.0000\ AB - 2.00\ AC - 1.25\ BC - 0.2750\ A^2 - 0.2750\ B^2 - 2.27\ C^2$
	$H_2 + CO = 29.00 + 13.87\ A - 1.37\ B + 3.50\ C - 1.25\ AB - 0.0000\ AC - 1.0000\ BC + 2.12\ A^2 + 0.6250\ B^2 - 3.12\ C^2$
Dolomite	$H_2 = 18.60 + 8.75\ A - 0.6250\ B + 1.38\ C + 1.25\ AB - 1.25\ AC + 0.5000\ BC - 2.80\ A^2 - 1.55\ B^2 - 2.55\ C^2$
	$H_2 + CO = 29.60 + 13.50\ A + 0.2500\ B + 1.50\ C - 0.5000\ AB - 0.5000\ AC + 1.50\ BC - 0.8000\ A^2 - 0.3000\ B^2 - 3.80\ C^2$

data with high accuracy as all R^2 values were in range of 0.98-0.99 which was closer to one. Additionally, the Adjusted R^2 values were also closer to R^2 values. The differences between R^2 and Adj R^2 were calculated, and 0.01 was obtained as the minimum difference and 0.02 as the maximum difference. According to [24], the difference values were small indicating the model is significant and good relation between experimental and predicted data. The blending ratio is the least effective on H_2, with a low F-value of 0.1477-4.37. The F-value was found in a range similar to the study [11], which is 0.67. The lack of fit values occurrence was due to low systematic errors from the experimental and model data [24].

Results of predicted and actual yield of H_2 and syngas for each catalyst were shown in Figure 6. All models show a good relationship between predicted value and actual value as the regression model accuracy was higher than 0.98.

Experimental Result

Effect of Catalyst

Figure 7 shows the relation between H_2 yields and catalyst loading at different temperatures. This graph aims to observe the differences between the lower and upper limits of catalyst loading, which are 0 wt% and 30 wt%, and their impact on product yields. At temperatures 700°C, 800°C and 900°C without the presence of a catalyst, the yield of H_2 obtained was 2 vol%, 12 vol% and 22 vol%, respectively. However, the addition of catalysts improves the H_2 yield from 7 vol% to 23 vol%. The highest H_2 yield was obtained at 900°C and 30 wt% of catalyst loading. The presence of a catalyst positively impacts hydrogen yield during the process, similar to the study from [11]. The catalyst's role was crucial in enhancing the efficiency of H_2-rich syngas production, making the process more effective.

H_2 Response in the Presence of Catalyst

Figure 8 shows the 3D response surface graphs for H_2 vol% with the combined effect of temperature, biomass ratio and catalyst loading. When two variables interact, the third variable was fixed at the middle value. Temperature varied from 700-900°C, three different biomass ratios (20SB:80OPF, 50SB:50SB and 80SB:20OPF) and 0%, 15% and 30% for catalyst loading for each limestone and dolomite. The 3D response graph in Figures 8a and 8d shows that the H_2 yield also increases as temperature increases. An increase in temperature from 700 to 900°C resulted in an H_2 yield increment of 2 vol% to 25 vol% and 24 vol% for limestone and dolomite, respectively. With limestone as

Table 6 ANOVA analysis for co-gasification using a natural catalyst

Source	Limestone				Dolomite			
	H_2 Vol%		H_2 + CO Vol%		H_2 Vol%		H_2 + CO Vol%	
	F-value	P-value	F-value	P-value	F-value	P-value	F-value	P-value
Model	112.55	< 0.0001	55.24	< 0.0001	59.46	< 0.0001	50.99	< 0.0001
Temperature	884.94	< 0.0001	444.57	< 0.0001	453.70	< 0.0001	430.63	< 0.0001
Biomass Ratio	1.94	0.2058	4.37	0.0750	2.31	0.1720	0.1477	0.7122
Catalyst	48.61	0.0002	28.29	0.0011	11.20	0.0123	5.32	0.0545
AB	0.000	1.0000	1.80	0.2211	4.63	0.0684	0.2954	0.6037
AC	27.65	0.0012	0.0000	1.0000	4.63	0.684	0.2954	0.6037
BC	10.80	0.0134	1.15	0.3182	0.7407	0.4179	2.66	0.1470
A2	0.0045	0.9481	5.49	0.0516	24.54	0.0017	0.7959	0.4019
B2	0.5504	0.4823	0.4748	0.5130	7.49	0.0290	0.1119	0.7478
C2	37.67	0.0005	11.87	0.0108	20.29	0.0028	17.96	0.0039
Residual	0.5786							
Lack of fit	1.08	0.0681	0.9762	0.4872	2.60	0.1889	2.10	0.2428
Pure Error	0.2000							
R^2	0.9931		0.9861		0.9871		0.9850	
Adj R^2	0.9843		0.9683		0.9705		0.9657	

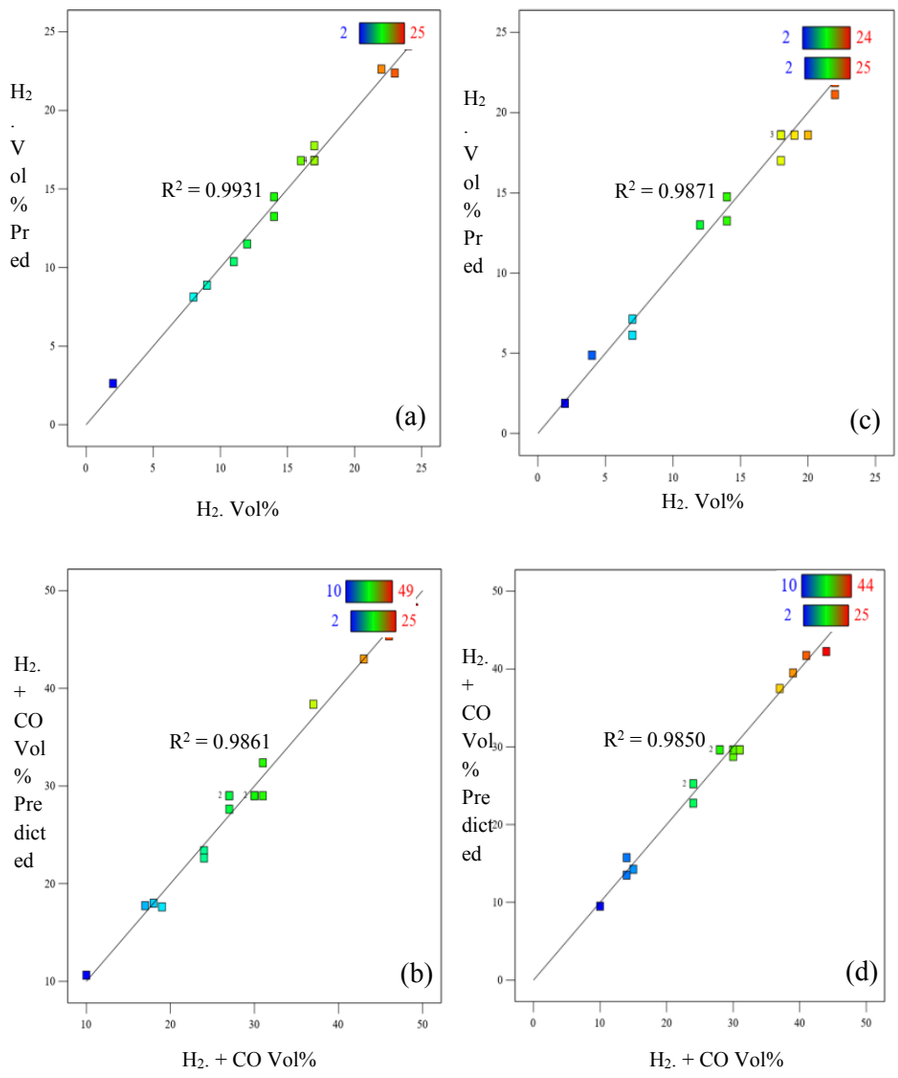

Figure 6 Actual vs predicted values of response from the respective model with (a,b) limestone and (c,d) dolomite

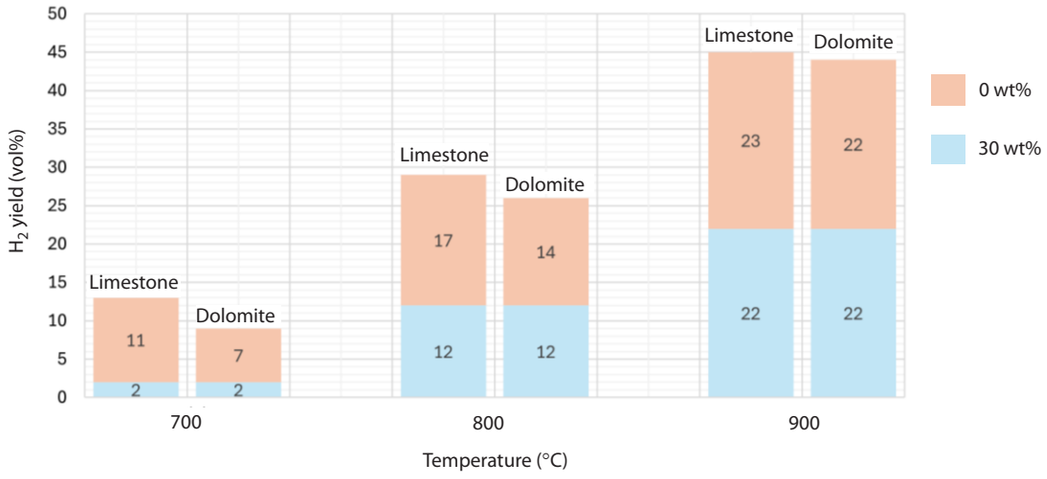

Figure 7 H_2 yield at different temperatures and catalyst loading

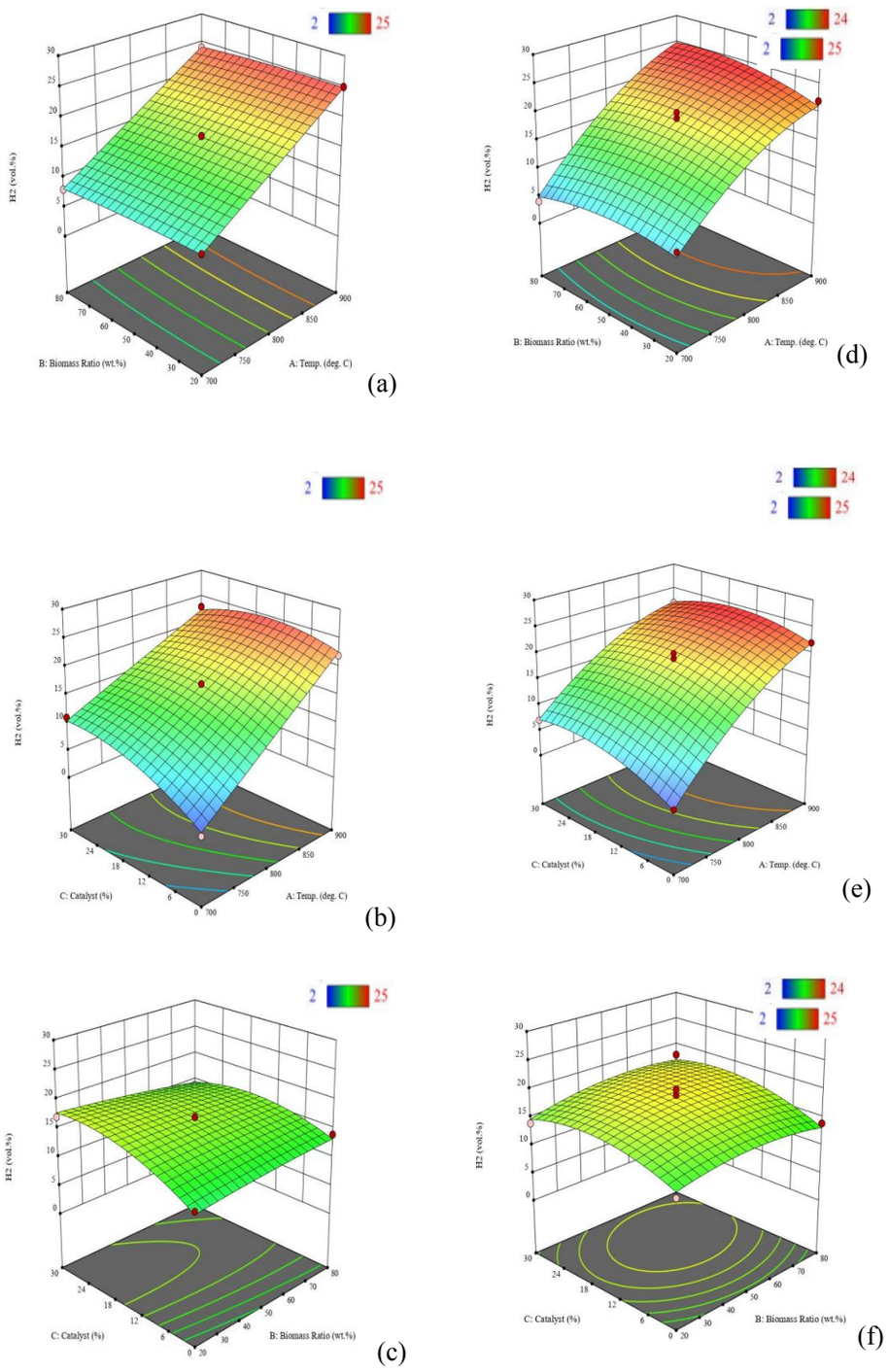

Figure 8 3D response surface graphs of H2 yield with the combined effect of the operating variables for (a-c) limestone and (d-f) dolomite

catalyst, the highest H_2 yield obtained was 25 vol% when temperature at 900°C and biomass ratio as 20SB:80OPF, compared to the lowest yield of 2 vol% without the presence of catalyst. According to Inayat et al. [24], the high value of H_2 yield might be due to the presence of catalytic activity from catalyst at high temperature. At the same parameters with the presence of dolomite, the H_2 yield obtained was 22 vol%. The highest H_2 yield with dolomite as the catalyst observed at temperature 900°C and 80SB:20OPF biomass ratio. This observation proves that high H_2 yield favours high temperature [25].

Figures 8b and 8e show the relationship between temperature and catalyst loading, with biomass ratio as the constant parameter. As the catalyst ratio increases, the H_2 yield also increases. From the discussion above, 900°C was concluded to be the favour in high H_2 yield. An increase in catalyst loading from 0 wt% to 15% resulted in an H_2 increment of 2 vol% to 25 vol% and 24 vol% for limestone and dolomite, respectively. Based on a study from [24], an increasing trend in H_2 yield was predicted with catalyst loading for any catalyst used. At temperature 900°C, with a catalyst loading of 15 wt%, the highest H_2 yield obtained for experiment runs with limestone and dolomite were 25 vol% and 24 vol%, respectively. The combined effect of biomass ratio and catalyst loading on H_2 yield can be depicted in Figures 8c and 8f. A 3D response plot of H_2 shows that the biomass ratio has no significant effect on the yield at the ranging value of catalyst loading. Based on the discussions, it was observed that H_2 yield was most influenced by temperature > catalyst loading > biomass ratio. Conclusively, limestone was found to be more effective in terms of H_2 production compared to dolomite catalysts. Under optimised conditions, limestone produced 25 vol% of hydrogen, followed by dolomite at 24 vol%.

Syngas Response in the Presence of Catalyst

The 3D surface and contour plots in Figure 9a-9f displayed the combination of input parameters' interrelation effect on H_2 + CO produced. Each graph illustrates the relationship between two parameters while the third parameter remained constant at its midpoint value. Figures 9a and 9c show the relation between temperature and biomass ratio on H_2 + CO yield for limestone and dolomite, respectively. The H_2 + CO yield increases as the temperature rises from 700-900°C, the temperature having a more significant influence. High operational temperature increases CO and H_2 content, enhances tar conversion, and promotes syngas production [26]. At 15 wt% catalyst loading, an increased temperature from 700 to 900°C resulted in H_2 + CO increment for both limestone and dolomite, from 17 vol% to 49 vol% and 14 vol% to 41 vol%, respectively.

Figures 9b and 9e demonstrate the mutual interaction between temperature and catalyst loading on H_2 + CO produced, with biomass ratio as the constant parameter. In this case, both catalysts show different ratios which had a more significant impact on H_2 + CO yield. For limestone, a higher OPF weightage in biomass ratio resulted in H_2 + CO yield increases from 17 vol% to 49 vol%. Meanwhile, a higher SB weightage in biomass ratio shows an increment in product yield from 15 vol% to 44 vol%. Moreover, Figures 9c and 9f displayed a 3D response plot of H_2 + CO. From the figures, both limestone and dolomite show that biomass ratio has a low significant effect on the yield at a ranging value of catalyst loading, which was similar to the previous observation of H_2 yield. The biomass ratio was found to have the least effect on the syngas because the composition of mixed materials and heating values do not vary as much as shown in Table 1 [11],[21]. Therefore, the biomass ratio has shown less effect on the co-gasification process. Based on the discussions, it was observed that H_2 + CO production was most influenced by temperature > catalyst loading > biomass ratio. According to [11], temperature was found to be the most influential factor that affects syngas production in the combined interaction of biomass blending ratio and catalyst loading. In conclusion, a higher H_2 + CO yield was obtained from limestone compared to dolomite. Under optimised conditions, limestone produced 49 vol% of H_2 + CO, followed by dolomite with 44 vol%.

Process Optimisation

The optimisation of temperature, biomass ratio, and catalyst for maximum H_2 in syngas production was carried out with the presence of natural catalysts, dolomite, and limestone. The variable range for the process optimisation to obtain the desired response output is shown in Table 7. The predicted and experimental values of H_2 and syngas yield are shown in Table 8. For limestone, the differences between predicted values and experimental values of H_2 and H_2 + CO were 0.55 vol% and 1.67 vol%, respectively. Meanwhile, for dolomite, the difference between predicted and experimental values of H_2 and syngas was 0.92 vol% and 1.74 vol%, respectively. The desirability of both natural catalysts was closer to unity, indicating a good relationship and reliable result between predicted values and experimental values. The solution with the highest yield was chosen as the best-optimised parameter, as shown in Figure 10 for the limestone catalyst and Figure 11 for the dolomite catalyst.

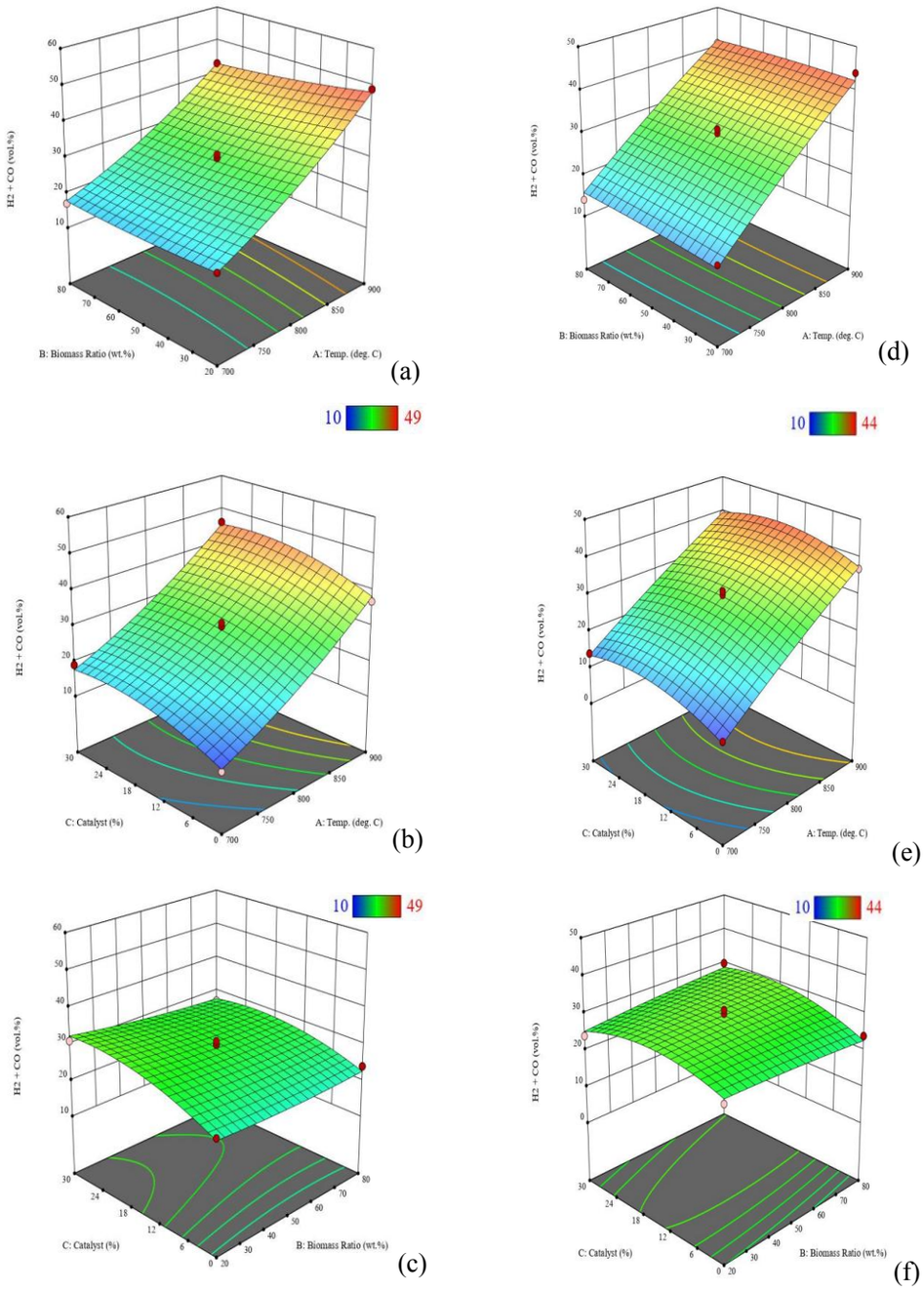

Figure 9 3D response surface graphs of H_2 + CO yield with the combined effect of the operating variables for (a-c) limestone and (d-f) dolomite

Table 7 Process optimisation within the variables for desired response output

Parameters	Range
A: Temperature	700-900°C
B: Biomass Ratio	20-80 wt%
C: Catalyst	0-30 wt%
H_2 vol%	Maximize
H_2 + CO vol%	Maximize

Table 8 Optimum process variables, predicted and confirmation data of responses

Catalyst	Conditions	Predicted values		Experimental values		Desirability
		H_2 (vol%)	H_2 + CO (%)	H_2 (vol%)	H_2 + CO (%)	
Limestone	Temp: 900°C Biomass Ratio: 20SB:80OPF Catalyst loading: 18%	25.01	49.06	25.56	50.73	1
Dolomite	Temp: 900°C Biomass Ratio: 45SB:55OPF Catalyst loading: 16%	24.15	42.37	25.07	44.11	0.976

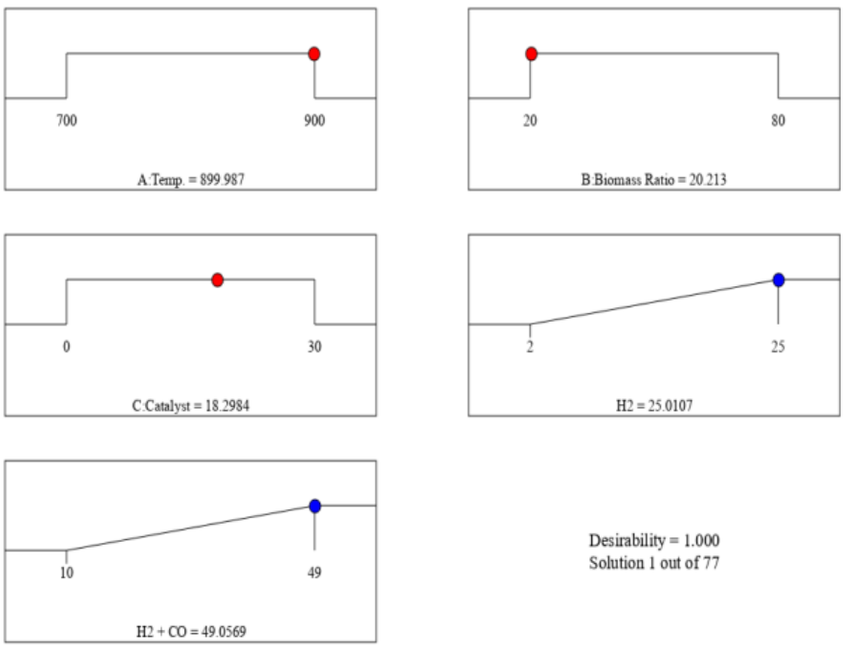

Figure 10 Desirability plot for H_2 and H_2 + CO produced from best-optimised parameters for imestone catalyst

CONCLUSION

Co-gasification proves to be a highly dependable method for oil and gas exploration. Its flexibility in choosing feedstock allows more research to be developed to produce syngas. By utilizing OPF and SB as feedstocks for co-gasification, the findings include that the data obtained with ANOVA and RSM showed that relation between the parameters was significant as the R^2 was closer to 1 and P-value <0.05. The presence of natural catalysts, dolomite and limestone act in improving hydrogen yields in final product. The yield of hydrogen/syngas was found to be influenced strongly by temperature. Based on the findings, it can be concluded that limestone is a better catalyst for producing H_2-rich syngas compared to dolomite. Under optimum conditions, the results expressed that maximum H_2 (25.56 – 25.07vol %) and syngas (44.11 – 50.73 vol%) yields were obtained at temperature 900°C, catalyst loading 18% (limestone); 16% (dolomite), and biomass ratio of 20SB:80OPF (limestone); 45SB:55OPF (dolomite). These findings provide valuable insight into the sustainable use of biomass waste for energy production.

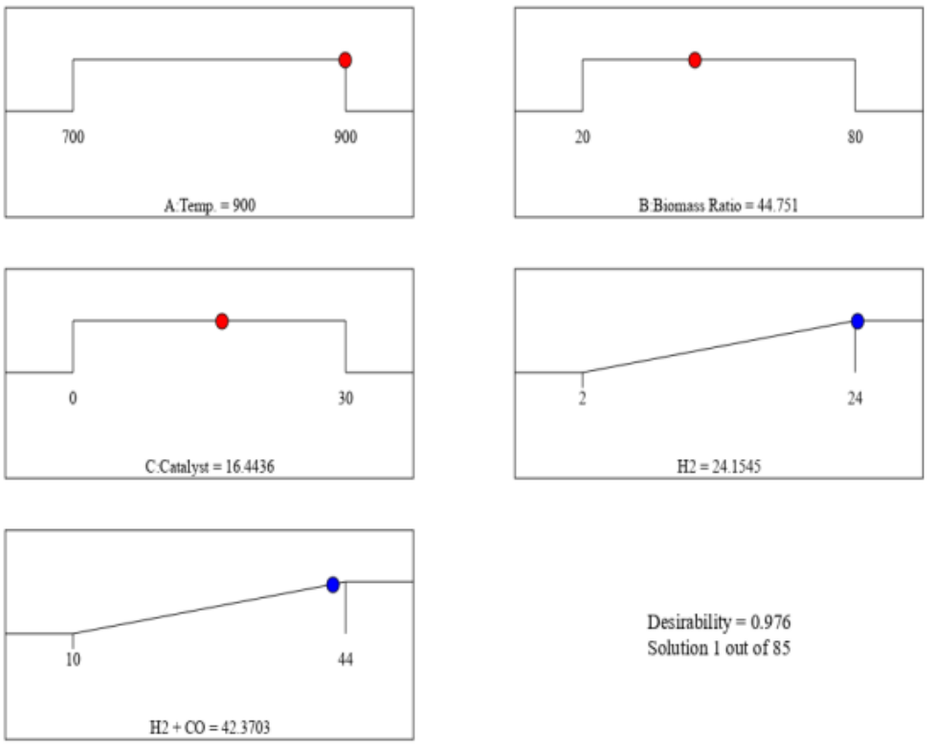

Figure 11 Desirability plot for H_2 and H_2 + CO produced from best-optimised parameters for Dolomite catalyst

ACKNOWLEDGMENT

The authors would like to sincerely thank Universiti Teknologi PETRONAS for financial support under grant number FRGS/1/2019/TK10/UTP/02/1. Also, the authors extend heartfelt thanks to Dr Kunmi Joshua Abioye and Dr Hayyiratul Fatimah for valuable insights and constructive feedback during the research process. Special thanks to the technical team, Mr Jailani Kassim, Mr Khairul and Mr Firdaus, for assistance with data collection and laboratory experiments. The authors also acknowledge FELCRA Nasaruddin Sdn Bhd Bota, Perak, Malaysia, for providing oil palm fronds for this work.

REFERENCES

[1] S. Mehariya, A. Iovine, P. Casella, D. Musmarra, A. Figoli, T. Marino, N. Sharma, and A. Molino, "Chapter 7 - Fischer–Tropsch synthesis of syngas to liquid hydrocarbons," in *Lignocellulosic Biomass to Liquid Biofuels*, Academic Press, 2020, pp. 217-248. doi: 10.1016/B978-0-12-815936-1.00007-1.

[2] S. Kanwal, M. T. Mehran, M. Hassan, M. Anwar, S. R. Naqvi, and A. H. Khoja, "An integrated future approach for the energy security of Pakistan: Replacement of fossil fuels with syngas for better environment and socio-economic development," *Renewable and Sustainable Energy Reviews,* vol. 156, 2022, Art. no. 111978, doi: 10.1016/j.rser.2021.111978.

[3] M. Inayat, S. A. Sulaiman, and J. C. Kurnia, "Catalytic co-gasification of coconut shells and oil palm fronds blends in the presence of cement, dolomite, and limestone: Parametric optimization via Box Behnken Design," *Journal of the Energy Institute,* vol. 92, no. 4, pp. 871-882, 2019, doi: 10.1016/j.joei.2018.08.002.

[4] N. E. H. Ali., "Agricultural waste management system [AWMS] in Malaysian," *Open Access Journal of Waste Management & Xenobiotics,* vol. 3 no. 2, pp. 000140, 2020, doi: 10.23880/oajwx-16000140

[5] N. Y. Harun, T. J. Han, T. Vijayakumar, A. Saeed, and M. T. Afzal, "Ash deposition characteristics of industrial biomass waste and agricultural residues," *Materials Today: Proceedings,* vol. 19, pp. 1712-1721, 2019, doi: 10.1016/j.matpr.2019.11.201.

[6] M. Ozturk, N. Saba, V. Altay, R. Iqbal, K. R. Hakeem, M. Jawaid, and F. H. Ibrahim, "Biomass and bioenergy:

An overview of the development potential in Turkey and Malaysia," *Renewable and Sustainable Energy Reviews,* vol. 79, pp. 1285-1302, 2017, doi: 10.1016/j.rser.2017.05.111.

[7] W. P. Q. Ng,, H. L. Lam, F. Y. Ng, M. Kamal, and J. H. E. Lim, "Waste-to-wealth: Green potential from palm biomass in Malaysia," *Journal of cleaner production,* vol. 34, pp. 57-65, 2012, doi: 10.1016/j.jclepro.2012.04.004.

[8] Z. Bo, L. Zhang, Z. Yang, and Z. He, "An experiment study of biomass steam gasification over NiO/Dolomite for hydrogen-rich gas production," *International Journal of Hydrogen Energy,* vol. 42, no. 1, pp. 76-85, 2017.

[9] M. Hu, L. Gao, Z. Chen, C. Ma, Y. Zhou, J. Chen, S. Ma, M. Laghari, B. Xiao, B. Zhang, and D. Guo,"Syngas production by catalytic in-situ steam co-gasification of wet sewage sludge and pine sawdust," in *Energy Conversion and Management,* vol. 111, Elsevier, 2016, pp. 409-416.

[10] K. Zakir, S. Yusup, M. M. Ahmad, and N. A. Rashidi, "Integrated catalytic adsorption (ICA) steam gasification system for enhanced hydrogen production using palm kernel shell," *International Journal of Hydrogen Energy,* vol. 39, no. 7, 2014.

[11] M. Inayat, S. A. Sulaiman, A. Inayat, N. B. Shaik, A. R. Gilal, and M. Shahbaz, "Modeling and parametric optimization of air catalytic co-gasification of wood-oil palm fronds blend for clean syngas (H2+ CO) production," *International Journal of Hydrogen Energy,* vol. 46, no. 59, pp. 30559-30580, 2021, doi: 10.1016/j.ijhydene.2020.10.268.

[12] S. A. Sulaiman, S. Balamohan, M. N. Z. Moni, S. M. Atnaw, and A. O. Mohamed, "Feasibility study of gasification of oil palm fronds," *Journal of Mechanical Engineering and Sciences,* vol. 9 , 2015, doi: 10.15282/jmes.9.2015.20.0168.

[13] G. Venkatesh, P. R. Reddy, and S. Kotari, "Generation of producer gas using coconut shells and sugar cane bagasse in updraft gasifier," *Materials Today: Proceedings,* vol. *4,* no. 8, pp. 9203-9209, 2017, doi: 10.1016/j.matpr.2017.07.278.

[14] M. W. Islam, "A review of dolomite catalyst for biomass gasification tar removal," *Fuel,* vol. 267, 2020, doi: 10.1016/j.fuel.2020.117095

[15] A. Gómez-Barea and B. Leckner, "Modeling of biomass gasification in fluidized bed," *Progress in Energy and Combustion Science,* vol. 36, no. 4, pp. 444-509, 2010, doi: 10.1016/j.pecs.2009.12.002.

[16] C. Dejtrakulwong and S. Patumsawad, "Four zones modeling of the downdraft biomass gasification process: Effects of moisture content and air to fuel ratio," *Energy Procedia,* vol. 52, pp. 142-149, 2014, doi: 10.1016/j.egypro.2014.07.064.

[17] Z. Ge, S. Guo, L. Guo, C. Cao, X. Su, and H. Jin, "Hydrogen production by non-catalytic partial oxidation of coal in supercritical water: explore the way to complete gasification of lignite and bituminous coal," *International Journal of Hydrogen Energy,* vol. *38,* no. 29, pp. 12786-12794, 2013, doi: 10.1016/j.ijhydene.2013.06.092.

[18] S. K. Sansaniwal, K. Pal, M. A. Rosen, and S. K. Tyagi, "Recent advances in the development of biomass gasification technology: A comprehensive review," *Renewable and Sustainable Energy Reviews,* vol. 72, pp. 363-384, 2017, doi: 10.1016/j.rser.2017.01.038.

[19] B. Prabir, *Biomass gasification and pyrolysis: Practical Design and Theory*, Academic Press, 2010, doi: 10.1016/C2009-0-20099-7

[20] S. Akshya, "Assessing the suitability of various feedstocks for biomass gasification," Louisiana State University and Agricultural & Mechanical College, 2011, doi: 10.31390/gradschool_theses.3758.

[21] K. J. Abioye, N. Y. Harun, S. Sufian, M. Yusuf, A. H. Jagaba, S. Waqas, and B. V. Ayodele, H. Kamyab, M. Alam, M. Gupta, H. S. Gill, S. Rezania, S. Chelliapan, and K. Kang, "Optimization of syngas production from co-gasification of palm oil decanter cake and alum sludge: An RSM approach with char characterization," *Environmental Research,* vol. 246, 2024, Art. no. 118027, doi: 10.1016/j.envres.2023.118027.

[22] L. Cao, K. M. Iris, X. Xiong, D. C. W. Tsang, S. Zhang, J. H. Clark, C. Hu, Y. H. Ng, J. Shang, and Y. S. Ok, "Biorenewable hydrogen production through biomass gasification: A review and future prospect," *Environmental Research*, vol. 186, 2020, Art. no. 109547, doi: 10.1016/j.envres.2020.109547.

[23] L. Zhou, Z. Yang, A. Tang, H. Huang, D. Wei, E. Yu, and W. Lu, "Steam-gasification of biomass with CaO as catalyst for hydrogen-rich syngas production," *Journal of the*

Energy Institute, vol. 92, no. 6, pp. 1641-1646, 2019, doi: 10.1016/j.joei.2019.01.010.

[24] A. Inayat, M. Inayat, M. Shahbaz, S. A. Sulaiman, M. Raza, and S. Yusup, "Parametric analysis and optimization for the catalytic air gasification of palm kernel shell using coal bottom ash as catalyst," *Renewable Energy,* vol. 145, pp. 671-681, 2020, doi: 10.1016/j.renene.2019.06.104

[25] K. J. Abioye, N. Y. Harun, S. Sufian, M. Yusuf, M. I. Khan, A. H. Jagaba, S. Sikiru, S. Waqas, H. Kamyab, A. M. Al-Enizi, S. S. Sehgal, M. Gupta, S. Rezania, and H. Ibrahim, "Kinetics and thermodynamic analysis of palm oil decanter cake and alum sludge combustion for bioenergy production," *Sustainable Chemistry and Pharmacy,* vol. 36, 2023, Art. no. 101306, doi: 10.1016/j.scp.2023.101306.

[26] D. A. Quintero-Coronel, Y. A. Lenis-Rodas, L. Corredor, P. Perreault, A. Bula and A. Gonzalez-Quiroga, "Co-gasification of biomass and coal in a top-lit updraft fixed bed gasifier: Syngas composition and its interchangeability with natural gas for combustion applications," *Fuel,* vol. 316, 2022, Art. no. 123394, doi: 10.1016/j.fuel.2022.123394.